

Single Nanowire Electrochemical Devices

Liqiang Mai,^{*,†,‡,§} Yajie Dong,^{*,†,§} Lin Xu,[†] and Chunhua Han[†]

[†]State Key Laboratory of Advanced Technology for Materials Synthesis and Processing, School of Materials Science and Engineering, Wuhan University of Technology, Wuhan, 430070, China, and [‡]Department of Chemistry and Chemical Biology, Harvard University, Cambridge, Massachusetts 02138

ABSTRACT We report the single nanowire electrode devices designed as a unique platform for in situ probing the intrinsic reason for electrode capacity fading in Li ion based energy storage devices. In this device, a single vanadium oxide nanowire or single Si/a-Si core/shell nanowire was used as working electrode, and electrical transport of the single nanowire was recorded in situ to detect the evolution of the nanowire during charging and discharging. Along with lithium ion intercalation by shallow discharge, the vanadium oxide nanowire conductance was decreased over 2 orders. The conductance change can be restored to previous scale upon lithium ion deintercalation with shallow charge. However, when the nanowire was deeply discharged, the conductance dropped over 5 orders, indicating that permanent structure change happens when too many lithium ions were intercalated into the vanadium oxide layered structures. Different from vanadium oxide, the conductance of a single Si/a-Si core/shell nanowire monotonously decreased along with the electrochemical test, which agrees with Raman mapping of single Si/a-Si nanowire at different charge/discharge states, indicating permanent structure change after lithium ion insertion and extraction. Our present work provides the direct relationship between electrical transport, structure, and electrochemical properties of a single nanowire electrode, which will be a promising and straightforward way for nanoscale battery diagnosis.

KEYWORDS Single nanowire electrodes, vanadium oxide, silicon, charge/discharge, electrical transport

Cathode and anode materials with high specific capacity are critical for high-energy lithium ion batteries with more and more extensive applications.^{1,2} As the two material systems with the highest theoretical capacities,¹ vanadium oxide based materials for cathodes or silicon for anodes are among the most promising materials for lithium ion storage. Unfortunately, they have long suffered from serious capacity fading issues upon cycling, which limits their commercialization.^{2–5}

Recently, nanostructured materials, especially nanowires, have attracted increasing interest and have been used in many energy related fields because of their unusual mechanical, electrical, optical, and piezoelectric properties endowed by confining the dimensions of such materials and because of the combination of bulk and surface properties to the overall behavior.^{6–10} Among them, vanadium oxide and silicon nanowire electrode materials have attracted increasing interest because they can offer a range of unique advantages over their traditional counterparts.^{6,11–18} Cui and co-workers have developed an electrode platform that uses silicon nanowires adhered to the current collector to accommodate the large volume change and to avoid capacity loss during cycling due to the decrepitation.^{6,11–15} Whittingham and co-workers have studied the evolution of the cycling ability of V₂O₅ with morphology changing from micro- to nanocrystalline and found that the capacity and

cycling stability of V₂O₅ nanorods are obviously superior to that of micro-V₂O₅.¹⁶

Single nanostructure devices have been exploited to demonstrate a powerful diagnostic tool, which allows for the direct correlation of the electrochemical property with the structure on the same nanoscale particle.¹⁹ Until now, however, the fundamental mechanisms of capacity fading and the direct relationship between electrical transport, structure and electrochemistry of vanadium oxide and silicon nanowire electrode materials, remain largely unexplored. This limitation is particularly critical for the development and optimization of high-energy density Li ion battery electrode materials. In the present work, we report fabrication of the smallest all-solid electrical energy storage devices using a simple design with just one nanowire. We will take it as a unique platform for in situ probing the direct correlation of electrical transport, structure, and electrochemistry to push the fundamental limits of the nanowire materials for energy storage applications.

We have employed a simple yet reliable design as schematically shown in Figure 1. It contains just one nanowire as either cathode or anode and uses classical materials for counter electrodes and electrolytes. No binders or conductive carbon additives were introduced into the systems. The design is also very effective in that it can provide insights on the intrinsic reason for electrode capacity fading which traditional battery test strategies cannot offer. Single nanostructure transport study can be combined with an electrode electrochemical performance test so that the relationship between electrode material composition, structure, transport properties, charge/discharge status, and electrochemical

* Corresponding authors, mlq@cmliris.harvard.edu and yjdong@cmliris.harvard.edu.

§ These authors contributed equally to this work.

Received for review: 08/12/2010

Published on Web: 09/10/2010



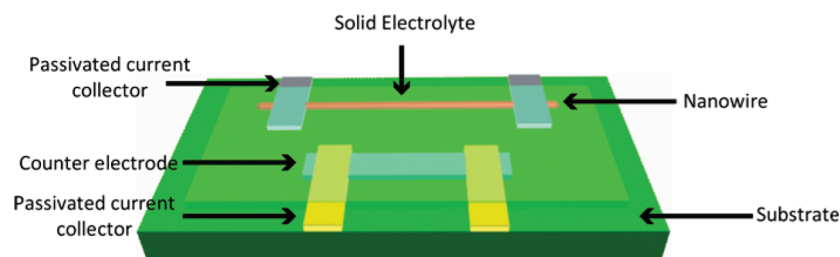


FIGURE 1. Schematic diagram of a single nanowire electrode device design. A single vanadium oxide nanowire or Si nanowire is the work electrode, and HOPG or LiCoO_2 nanofilm is the counter electrode. The electrolyte is the PEO- LiClO_4 -PC-EC polymer.

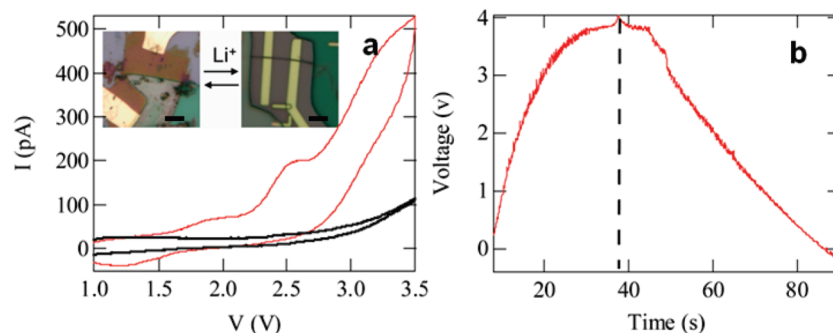


FIGURE 2. Electrochemistry of single $\text{V}_3\text{O}_7 \cdot \text{H}_2\text{O}$ nanowire electrode device. (a) Cyclic voltammogram (C-V) of single vanadium oxide nanowire from 1.0 to 3.5 V versus HOPG at 50 mV/s scan rate: black, control C-V using only Cr/Au pad against HOPG; red, C-V of a typical vanadium oxide NW cathode/HOPG anode. Insets show the optical micrograph images of a typical HOPG (left) and a vanadium oxide nanowire (right) device (scale bars are 5 μm). (b) Voltage profile of a single vanadium oxide nanowire cathode versus HOPG during charge and discharge (charged at -150 pA and discharged at 50 pA).

performance can be studied at a single nanowire level to reveal the intrinsic reason for fast capacity fading.

For a nanowire cathode study, vanadium oxide ($\text{V}_3\text{O}_7 \cdot \text{H}_2\text{O}$) nanowire was chosen as an example. Vanadium oxide nanowires were successfully prepared by hydrothermal reaction^{20,21} using V_2O_5 sol.²² Briefly, 1.3 mmol of the as-prepared V_2O_5 sol, 3.6 μL of aniline, and 0.04 g of poly(ethylene glycol) (PEG) ($M_w = 4000$) were mixed by stirring and then transferred into a Teflon-lined stainless steel autoclave and kept at 180 °C for 2 days. The products were collected and washed repeatedly with distilled water, and finally dried at 80 °C in air for 12 h. Figure S1 in the Supporting Information shows structure characterization of the as-prepared $\text{V}_3\text{O}_7 \cdot \text{H}_2\text{O}$ nanowires. The X-ray diffraction (XRD) pattern of the as-synthesized products can be assigned to the phase of $\text{V}_3\text{O}_7 \cdot \text{H}_2\text{O}$ orthorhombic structure, which is in good agreement with JCPDS card 85-2401. The vanadium oxide nanowires are with length of 10–45 μm and diameter of 20–100 nm. Electrochemical tests demonstrated that vanadium oxide nanowires have high initial discharge capacity of ~400 mAh/g although they suffer from fast capacity fading after the first several cycle tests,²³ a typical behavior for vanadium oxide based cathode materials.

Our vanadium oxide nanowire electrode device was configured with one nanowire as cathode, one flake of highly ordered pyrolytic graphite (HOPG) as anode, and polymer (poly(ethylene oxide) (PEO), LiClO_4 , propylene carbonate (PC)/ethylene carbonate (EC) 20 mol %) ^{24a} as electrolytes.

We first dry transferred HOPG flakes onto a marked substrate and then deposit vanadium oxide nanowires onto the region close to the HOPG flakes followed by current collector patterning with e-beam lithography and deposition of Cr/Au (10/100 nm) and Si_3N_4 layer (300 nm) with thermal evaporator and PECVD, respectively. Finally, a polymer electrolyte was drop cast onto the marked region to finish up the device fabrications. Compared to single vanadium oxide nanowire, the HOPG flake has much larger surface area, on which the influence is little during electrochemical test. Therefore, the electrochemical test data are controlled by the cathode nanowire, and the polarization of HOPG anode can be neglected. The cyclic voltammogram (C-V) of the vanadium oxide nanowire electrode is shown in Figure 2a together with a control C-V between HOPG and blank passivated Cr/Au current collectors without nanowire. It is clear that the typical oxidation and reduction peaks were only observed with the vanadium oxide nanowire electrode with current around four to five times that of the control, indicating that lithium ion is intercalating and deintercalating into the nanowire.

For a battery performance test, a galvanostat is often employed to apply a constant current to charge or discharge a battery and meanwhile monitor the voltage between the working and reference electrodes. A high precision measurements setup can determine Coulombic efficiency accurately and provide insight on battery parasitic reactions and are thus of importance for research and development of Li-ion batteries.^{24b} In our case, because the very small

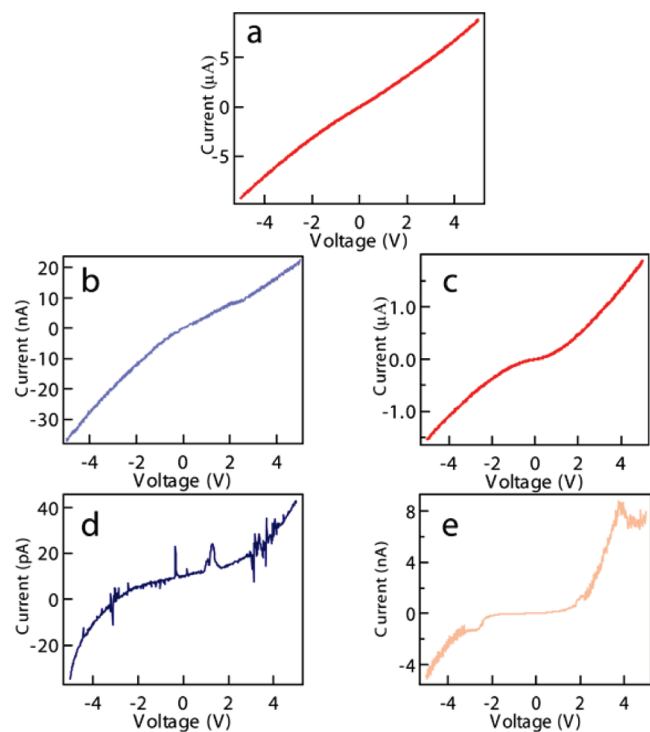


FIGURE 3. Single vanadium oxide nanowire transport properties at different charge/discharge states: (a) initial state; (b) after Li^+ ion intercalation (shallow discharge with 100 pA for 200 s); (c) after Li^+ ion deintercalation (shallow charge with -100 pA for 200 s); (d) after deep discharge with 100 pA for 400 s; (e) after deep charge with -100 pA for 400 s.

current level (estimated at \sim tens of pica-amperes) and very high internal impedance (estimated at \sim tens of gigaohms) may be well beyond or close to the limits most galvanostats can provide, we have assembled a setup for measurement with a constant current source (Keithley 6220, with current down to 100 fA) and an ultrahigh internal impedance voltmeter (Trek 800 InfiniTron, with internal impedance $>10^{16} \Omega$) together with the probe station (Desert TTP4) by BNC or triaxial cables. Figure 2b shows the voltage profile of one charge/discharge cycle of a vanadium oxide nanowire cathode versus HOPG anode. Along with charge using -150 pA, the cell voltage increases and is saturated at around 3.9 V. The voltage then dropped back with a sloping profile when being discharged at 50 pA. The slope profile is an indication that the cell has either a very high internal resistance or high discharging rate.²⁵

During battery charge or discharge, Li^+ ions move out or into the cathode materials, oxidizing or reducing it to different states. This process was usually studied ex situ after disassembling the battery.^{6b} So far, only in situ XRD^{26a} or NMR^{26b,c} could provide some indirect hint on materials structure changes during the battery test. Our single nanowire battery design provides a unique advantage to study this in situ without disturbing the battery components.

Figure 3 shows the transport properties of the same single nanowire at different charge/discharge status. Initially, the

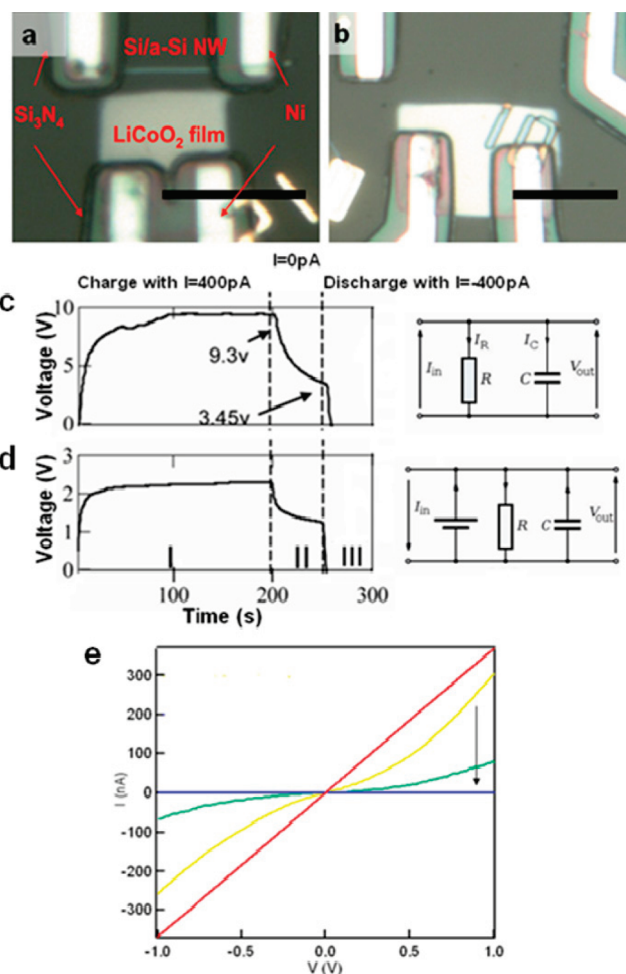


FIGURE 4. Single Si/a-Si core/shell nanowire electrode study. Optical images of a typical Si/a-Si nanowire/ LiCoO_2 electrode device (a) and control device (b) that has the same electrode design but without Si/a-Si nanowires. Scale bar is $10 \mu\text{m}$. Charge/discharge behavior and equivalent circuits for each setup of (c) control with LiCoO_2 electrode versus blank passivated Cr/Au current collector and (d) LiCoO_2 electrode versus single Si/a-Si nanowire electrode. The compliant voltage for the constant current source is 10 V. (e) Transport property evolution of Si/a-Si nanowire along with electrochemical test: red, initial state/100; yellow, after first cycle; green, after 10 min, 400 pA charge; blue, after 10 min, -400 pA discharge.

vanadium oxide nanowire was highly conductive (Figure 3a), agreeing with its original intact crystal structures. Along with lithium ion intercalation by shallow discharge with 100 pA for 200 s, the nanowire conductance was decreased over 2 orders (Figure 3b). The conductance change can be restored to previous scale upon Li^+ ion deintercalation with shallow charge with -100 pA for 200 s (Figure 3c) indicating reversible structure change. However, when the battery device was deeply discharged with 100 pA for 400 s, the nanowire conductance dropped over 5 orders (Figure 3d). This change was permanent and could not be recovered even after deep charging with -100 pA for 400 s, indicating that permanent structure change happens when too many lithium ions were intercalated into the vanadium oxide layered structures. Here, the material electrical properties,

crystal structure change, and electrochemical charge/discharge status are clearly correlated on the single nanowire electrode platform.

For a silicon-based anode nanowire study, we are focusing on a Si/a-Si core/shell nanowire with the expectation that the crystalline core will work as the conducting path while a disordered a-Si structure can accommodate more strain than ordered crystalline Si during Li diffusion in and out. The counter cathode electrodes LiCoO₂ thin films were deposited onto the e-beam lithography patterned region by magnetron sputtering with their position and spacing to the nanowire precisely controlled (Figure 4a). The device fabrication was carried out on a quartz substrate instead of silicon since we hope to do some Raman characterization on silicon nanowire devices without worrying about the disturbance from substrates. To single out the exact effect from the nanowire, we also designed a control device (Figure 4b), for which everything else is the same except that no nanowire was used. The transport properties of both LiCoO₂ cathode and Si/a-Si nanowire anode were tested before and after applying polymer electrolytes. Upon polymer electrolyte immersion, the conductivity of a Si/a-Si nanowire decreased to one-quarter as before (Figure S2a in the Supporting Information). Conductivity of the LiCoO₂ film is low compared to reported data²⁷ and might need further improvement in the future (Figure S2b in the Supporting Information).

Si/a-Si nanowire anode performance was tested together with careful control experiments. First, the control device with LiCoO₂ electrode versus blank passivated Cr/Au current collector (Figure 4c) can be regarded as a RC circuit. The real

single nanowire anode device, as modeled in Figure 4d, can be regarded as an ideal battery in parallel with a RC circuit. A closer examination of parts c and d of Figure 4c reveals the sloping behavior of both discharge curves. This linear behavior is representative of a typical capacitive discharge. Generally, the total stored charge in a Li-based electrochemical device can be separated into three components: the Faradaic contribution from diffusion controlled Li⁺ insertion, the Faradaic contribution from electrosorption and surface redox processes (so-called pseudocapacitance), and the non-Faradaic contribution from the double-layer capacitance.^{1f,28} The CV curve of real Si/a-Si single nanowire anode device (yellow curve in Figure S3 in the Supporting Information) reveals broad peaks. This is characteristic of a surface-confined charge-transfer process, which indicates that the stored charge is mainly pseudocapacitive in nature. Notably, the slope profile in discharge curve (Figure 2b) and broad peak characteristics of CV curve (Figure 2a) for single vanadium oxide nanowire cathode also show certain pseudocapacitive discharge. Similar behavior has also been reported for other host materials with layered crystalline structure.^{29,30} Considering the present single nanowire device design and performance, we believe that optimizing the passivation layer, reducing the contact area of electrolyte and passivated current collectors, and improving LiCoO₂ cathode thin film conductivity will probably be effective ways to increase the ratio of Faradaic contribution to non-Faradaic contribution and gain better battery performance.

The transport properties of the Si/a-Si core/shell nanowire at different charge/discharge status were characterized im-

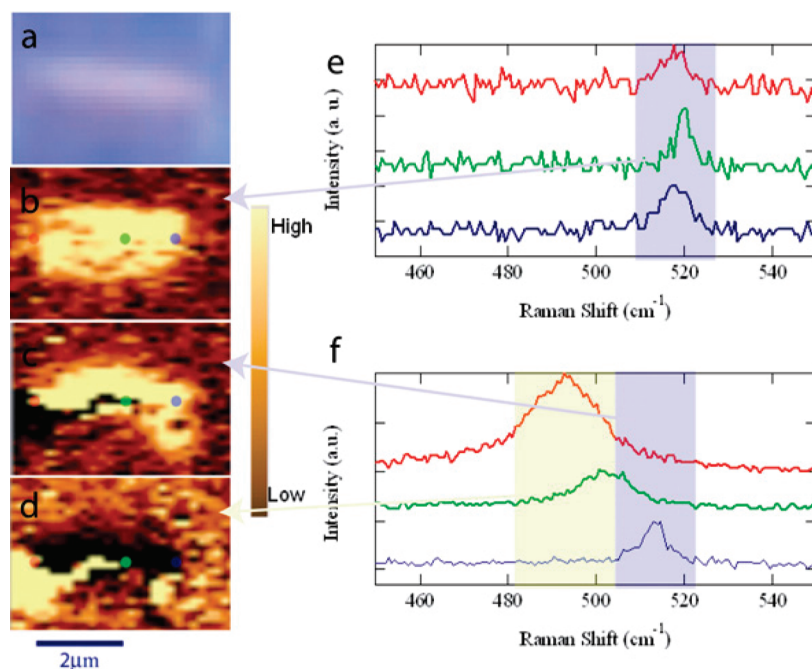


FIGURE 5. Raman mapping of Si/a-Si nanowire electrode device before and after electrochemical cycling. (a) Optical image of nanowire device, Raman mapping before (b) and after (c, d) electrochemical cycling. The Raman spectra of the three spots denoted in (b–d) are displayed in (e) and (f). The shaded area is the region employed for respective Raman mapping.

mediately after the electrochemical performance test. Interestingly, instead of reversible change, the conductance of the nanowire monotonously decreased along with electrochemical cycling (Figure 4e). After the initial charge/discharge cycle, the conductance of the nanowire decreased for over 2 orders. This observation agrees with what has been reported in literature,^{6a,31} indicating similar permanent structure change, such as silicon amorphization³¹ after lithium insertion and extraction. Our result on transport degradation is in excellent agreement with the capacity decrease along with electrochemical test indicated by CV investigation (Figure S3 in the Supporting Information).

To further reveal the structure change at the single nanowire level, we characterized the nanowire anode with confocal Raman microscopy (WITec CRM-200). Figure 5 shows the Raman mapping results of single nanowire anode together with the Raman spectra of highlighted spots at different charge states. Before electrochemical performance test, the nanowire has identical Raman spectra with characteristic Si peaks at $\sim 520\text{ cm}^{-1}$ at different spots (Figure 5b,e). After electrochemical cycling, the Raman mapping became not uniform any more with a threadlike region developed from one current collector contact (Figure 5c,d). The corresponding Raman spectra showed clear red shifts (514, 503, 493 cm^{-1}) and broadening (fwhm, 7, 13, 19 cm^{-1}) because crystalline silicon lost its order and became metastable amorphous Li_xSi alloy.^{6b} This observation clearly explained the conductance degradation discussed in Figure 4e.

In conclusion, we have reported a study of vanadium oxide based cathode and silicon based anode at the single nanowire level and demonstrated that a single nanowire electrode can work as a versatile platform to study the correlation between material structure changes, transport property, and electrochemical property. The insight gained from this study could help understand the intrinsic mechanism of battery capacity fading of these two promising material systems. It was found that conductivity of the nanowire electrode decreased reversibly (for vanadium oxide nanowire by shallow discharge/charge) or irreversibly (for vanadium oxide nanowire by deep discharge/charge, or silicon nanowire) during the electrochemical reaction, which limits the cycle life of the devices. A key issue for improving the performance of lithium ion batteries is to restrain the conductivity decrease of the electrode materials, such as prelithiation in our previous work.^{32,33} Meanwhile, a single nanowire energy storage device is promising for nanoscale battery diagnosis and has the potential to provide the power needs of nanodevices to build self-powered nanosystems.

Acknowledgment. This work was partially supported by the National Nature Science Foundation of China (50702039, 51072153), the Research Fund for the Doctoral Program of Higher Education (20070497012), the Fundamental Research Funds for the Central Universities (2010-II-016), and Scientific Research Foundation for Returned Scholars, Min-

istry of Education of China (2008-890). We express our deep thanks to Professor C. M. Lieber of Harvard University for his careful supervision, strong support, and stimulating discussion. We also thank Professor Y. Shao of Massachusetts Institute of Technology for her helpful discussion.

Supporting Information Available. Figures showing structure characterization of vanadium oxide nanowires, typical $I-V$ curves of Si/a-Si nanowire anode and LiCoO_2 cathode before and after applying polymer electrolytes, and cyclic voltammogram evolution of Si/a-Si nanowire along with electrochemical test. This material is available free of charge via the Internet at <http://pubs.acs.org>.

REFERENCES AND NOTES

- (1) (a) Tarascon, J. M.; Armand, M. *Nature* **2001**, *414*, 359. (b) Kang, K.; Meng, Y. S.; Berger, J.; Grey, C. P.; Ceder, G. *Science* **2006**, *311*, 977. (c) Nam, K. T.; Kim, D. W.; Yoo, P. J.; Chiang, C. Y.; Meethong, N.; Hammond, P. T.; Chiang, Y. M.; Belcher, A. M. *Science* **2006**, *312*, 885. (d) Huang, Y. H.; Goodenough, J. B. *Chem. Mater.* **2008**, *20*, 7237. (e) Kang, B.; Ceder, G. *Nature* **2009**, *458*, 190. (f) Lee, S. W.; Yabuuchi, N.; Gallant, B. M.; Chen, S.; Kim, B. S.; Hammond, P. T.; Shao, Y. *Nat. Nanotechnol.* **2010**, *5*, 531.
- (2) Whittingham, M. S. *J. Electrochem. Soc.* **1976**, *123*, 315.
- (3) Wen, C. J.; Huggins, R. A. *J. Solid State Chem.* **1976**, *37*, 271.
- (4) Zavalij, P. Y.; Whittingham, M. S. *Acta Crystallogr., Sect. B* **1999**, *55*, 627.
- (5) Boukamp, B. A.; Lesh, G. C.; Huggins, R. A. *J. Electrochem. Soc.* **1981**, *128*, 725.
- (6) (a) Chan, C. K.; Peng, H.; Liu, G.; McIlwrath, K.; Zhang, X. F.; Huggins, R. A.; Cui, Y. *Nat. Nanotechnol.* **2008**, *3*, 31. (b) Li, H.; Huang, X. J.; Chen, L. Q.; Zhou, G. W.; Zhang, Z.; Yu, D. P.; Mo, Y. J.; Pei, N. *Solid State Ionics* **2000**, *135*, 181.
- (7) Tian, B. Z.; Zheng, X. L.; Kempa, T. J.; Fang, Y.; Yu, N. F.; Yu, G. H.; Huang, J. L.; Lieber, C. M. *Nature* **2007**, *449*, 885.
- (8) Dong, Y. J.; Tian, B. Z.; Kempa, T. J.; Lieber, C. M. *Nano Lett.* **2009**, *9*, 2183.
- (9) Xu, S.; Qin, Y.; Xu, C.; Wei, Y.; Yang, R.; Wang, Z. L. *Nature Nanotechnol.* **2010**, *5*, 366.
- (10) Lieber, C. M.; Wang, Z. L. *MRS Bull.* **2007**, *32*, 99.
- (11) Cui, L. F.; Ruffo, R.; Chan, C. K.; Peng, H.; Cui, Y. *Nano Lett.* **2009**, *9*, 491.
- (12) Cui, L. F.; Yang, Y.; Hsu, C. M.; Cui, Y. *Nano Lett.* **2009**, *9*, 3370.
- (13) Chan, C. K.; Ruffo, R.; Hong, S. S.; Huggins, R. A.; Cui, Y. *J. Power Sources* **2009**, *189*, 34.
- (14) Ruffo, R.; Hong, S. S.; Chan, C. K.; Huggins, R. A.; Cui, Y. *J. Phys. Chem. C* **2009**, *113*, 11390.
- (15) Chan, C. K.; Peng, H.; Twisten, R. D.; Jarausch, K.; Zhang, X. F.; Cui, Y. *Nano Lett.* **2007**, *7*, 490.
- (16) Chernova, N. A.; Roppolo, M.; Dillon, A. C.; Whittingham, M. S. *J. Mater. Chem.* **2009**, *19*, 2526.
- (17) Chen, W.; Peng, J. F.; Mai, L. Q.; Yu, H.; Qi, Y. Y. *Chem. Lett.* **2004**, *33*, 1366.
- (18) Chen, W.; Mai, L. Q.; Qi, Y. Y.; Dai, Y. *J. Phys. Chem. Solids* **2006**, *67*, 896.
- (19) (a) Campbell, J. K.; Sun, L.; Crooks, R. M. *J. Am. Chem. Soc.* **1999**, *121*, 3779. (b) Heller, I.; Kong, J.; Heering, H. A.; Williams, K. A.; Lemay, S. G.; Dekker, C. *Nano Lett.* **2005**, *5*, 137. (c) Yang, Y.; Xie, C.; Ruffo, R.; Peng, H.; Kim, D. K.; Cui, Y. *Nano Lett.* **2009**, *9*, 4109.
- (20) Zhang, S.; Li, W.; Li, C.; Chen, J. *J. Phys. Chem. B* **2006**, *110*, 24855.
- (21) Chirayil, T.; Zavalij, P. Y.; Whittingham, M. S. *Chem. Mater.* **1998**, *10*, 2629.
- (22) Vanadium oxide nanowires were synthesized as follows: V_2O_5 powder was heated to 800 °C in a ceramic crucible. When the molten liquid was quickly poured into distilled water, a brownish V_2O_5 sol was formed. Then 1.3 mmol of the as-prepared V_2O_5 sol, 3.6 μL of aniline, and 0.04 g of poly(ethylene glycol) (PEG) ($M_w = 4000$) were mixed by stirring, and then transferred into a

Teflon-lined stainless steel autoclave and kept at 180 °C for 2 days. Then the autoclave was allowed to cool down in air, and the green precipitate was obtained. The products were collected, washed repeatedly with distilled water, and finally dried at 80 °C in air for 12 h.

- (23) Gao, S.; Chen, Z.; Wei, M.; Wei, K.; Zhou, H. *Electrochim. Acta* **2009**, *54*, 1115.
- (24) (a) Agrawal, R. C.; Pandey, G. P. *J. Phys. D: Appl. Phys.* **2008**, *41*, 223001. (b) Smith, A. J.; Burns, J. C.; Trussler, S.; Dahn, J. R. *J. Electrochem. Soc.* **2010**, *157*, 196.
- (25) Linden, D.; Reddy, T. B. *Handbook of batteries*; McGraw-Hill: New York, 2004.
- (26) (a) Yoon, W. S.; Chung, K. Y.; Balasubramanian, M.; Hanson, J.; McBreen, J.; Yang, X. Q. *J. Power Sources* **2006**, *163*, 219. (b) Key, B.; Bhattacharyya, R.; Morcrette, M.; Seznec, V.; Tarascon, J.-M.; Grey, C. P. *J. Am. Chem. Soc.* **2009**, *131*, 9239–9249. (c) Bhattacharyya, R.; Key, B.; Morcrette, M.; Chen, H. L.; Best, A. S.; Hollenkamp, A. F.; Grey, C. P. *Nat. Mater.* **2010**, *9*, 504–510.
- (27) Wei, G.; Haas, T. E.; Goldner, R. B. *Solid State Ionics* **1992**, *58*, 115.
- (28) (a) Winter, M.; Brodd, R. J. *Chem. Rev.* **2004**, *104*, 4245. (b) Brezesinski, T.; Wang, J.; Tolbert, S. H.; Dunn, B. *Nat. Mater.* **2010**, *9*, 146.
- (29) Zúkalova, M.; Kalbac, M.; Kavan, L.; Exnar, I.; Graetzel, M. *Chem. Mater.* **2005**, *17*, 1248.
- (30) Li, J. R.; Tang, Z. L.; Zhang, Z. T. *Chem. Mater.* **2005**, *17*, 5848.
- (31) Zhou, G. W.; Li, H.; Sun, H. P.; Yu, D. P.; Wang, Y. Q.; Huang, X. J.; Chen, L. Q.; Zhang, Z. *Appl. Phys. Lett.* **1999**, *75*, 2447.
- (32) Mai, L. Q.; Hu, B.; Chen, W.; Qi, Y. Y.; Lao, C. S.; Yang, R. S.; Wang, Z. L. *Adv. Mater.* **2007**, *19*, 3712.
- (33) Mai, L. Q.; Xu, L.; Hu, B.; Gu, Y. H. *J. Mater. Res.* **2010**, *25*, 1413.